Zeitschrift: Schweizer Archiv für Tierheilkunde SAT : die Fachzeitschrift für Tierärztinnen und Tierärzte = Archives Suisses de Médecine Vétérinaire ASMV : la revue professionnelle des vétérinaires

Herausgeber: Gesellschaft Schweizer Tierärztinnen und Tierärzte

Band: 132 (1990)

Heft: 8

Artikel: Natural acanthamoeba infection in greyhound dogs

Autor: Buergelt, C.D. / Harrison, L.R. / Liggett, A.D.

DOI: https://doi.org/10.5169/seals-592970

Fig. 1. Group I: Seminiferous duct with immature spermatids.
Fig. 2. Group II: Immature binucleated spermatidy with poor developed Golgi complex; fragmented chromatoid body.

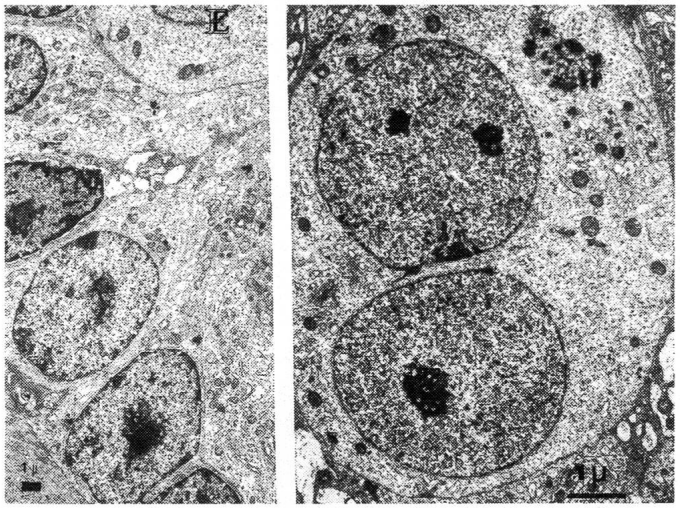

The anomalies found in the cytoplasmic organellae prevented spermatozoal development. We want to emphasize the fact that fragmentations in the chromatoid bodies prevented the formation of flagellae. Although further evidence may be required, we believe that undifferentiated spermatids are a sign of tumour development of the seminiferous epithelium due to extended treatment with anabolic hormones.

Table 1.

	lots	animals	sacrifice age	inoculated time
experimental	I	6	75 days	30 days
group	II	6	105 days	60 days
control	I	6	75 days	
group	II	6	105 days	

References

1. Bellido C., Gaytan F. (1985): Biol Reprod vol. *33*, 381–387. — *2. Hoffman B.* (1986): Agora ONE. Jornadas Técnicas de vacuno de carne. Palacio de Cristal, Lérida, 30 Mayo–2 de Junio de 1986. — *3. Michel G., Baulieu E. E.* (1983): En: Anabólicos en Producción Pecuaria, Simposio celebrado en la O.I.E. pág. 55–66, Paris 1983. — *4. Rao MV, Chinoy NJ* (1984): Exp Clin Endocrinol *34*, 211–217. — *5. Wiggins JP* et al. (1980): Am J Vet Res vol. *41*, 487–492.

Div. Experimental Pathology, Inst. Animal Pathology, University of Berne

HYPOTHALAMO-PITUITARY-GONADAL AXIS OF AGED FEMALE RATS. A FUNCTIONAL AND MORPHOLOGICAL STUDY

C. E. Boujon, G. E. Bestetti, M. J. Reymond, G. L. Rossi

Median eminence (ME) and mediobasal hypothalamus (MBH) LHRH and plasma FSH, LH, and progesterone were measured by RIA in young diestrus (age 3 months) and old recurrently pseudopregnant (RPP; age 23–24 months) female Long-Evans rats. Lateral ME (LME) LHRH as well as pituitary FSH and LH contents were also evaluated by morphometry and densitometrical immunocytochemistry. Further, by light microscopy we classified and counted the number of ovarian follicles and corpora lutea.

By RIA hypothalamic LHRH, plasma LH and progesterone were similar in the two groups while plasma FSH was higher in old than in young animals. The number of LHRH-labeled axons was reduced in the LME of old rats. Further, the pattern of pixel distribution into classes of increasing gray levels was different in the two groups. The number of nucleated FSH-labeled cells and the total FSH area and immunoreactivity were almost twice in old compared with young animals. The measurements of LH-labeled cells were not different in the two groups. In old rats the number of ovarian follicles and corpora lutea was reduced and that of atretic follicles increased.

In conclusion, our data indicate that decreased LME LHRH associated with increased FSH-gonadotropes and plasma FSH occur in old RPP rats. These changes may contribute to explain the complex hormonal disarrangement responsible for the decline of reproductive functions in old female rats.

Dep. Compar. & Experim. Pathology, College of Vet. Med., University of Florida, Gainesville

NATURAL ACANTHAMOEBA INFECTION IN GREYHOUND DOGS

C. D. Buergelt, L. R. Harrison, A. D. Liggett, R. W. Bauer

Naturally occurring epizootics of acanthamoebiasis were diagnosed on six geyhound farms from Northern Florida and Southern Georgia. Three of the outbreaks occurred in the summer and fall of 1985 and 3 more happened in the summer of 1988. The dogs affected ranged in age from 8 weeks to 13 months, with clustering in the 5 to 7 month range. Clinical signs included oculonasal discharge, anorexia, lethargy, coughing, dyspnea, hemoptysis and neurologic disturbances. Cadavers and tissues from 14 cases were examined. Gross necropsy findings included acute, multifocal, nectrotizing pneumonia, and/or multifocal, hemorrhagic meningoencephalitis. Microscopically, a necrohemorrhagic pneumonia with an interstitial pattern and numerous protozoal organisms resembling amebic trophozoites were diagnosed. Brain lesions were multifocal granulomas with vasculitis and necrosis. Amebic organisms similar to these in the lung were present within the necrotic cerebral foci. Lesions in other tissues were

not consistently seen, but granulomas generally associated with trophozoites in glomeruli of some puppies were noted. The light-microscopic findings were supported by electron-microscopic findings of amebic trophozoites in brain and lung samples. Direct immunofluorescence performed at the Centers for Disease Control in Atlanta, Georgia, on lung and brain samples identified the amebic organisms to belong to the genus *Acanthamoeba*. *Acanthamoeba* provide a diagnostic challenge in that they are difficult to differentiate from certain mammalian cells, especially macrophages. The diagnostic feature of *Acanthamoeba* in histopathologic sections is the central nucleolus. Specific laboratory procedures are generally necessary to confirm *Acanthamoeba* infection.

Dpto. Anatomía y Anatomía Patológica, Córdoba, Spain

INTRAVASCULAR MACROPHAGES IN THE LUNG OF RABBITS WITH EXPERIMENTAL VIRAL HAEMORRHAGIC DISEASE

L. Carrasco, J. C. Gómez-Villamandos, E. Díaz, J. B. Poveda, A. Fernández

The haemorrhagic viral disease (HVD) occurring in rabbits is characterized by severe necrotic hepatitis and congestive-haemorrhagic phenomena affecting different organs including the lungs (4). It is usually diagnosed on liver and lung samples, which usually show the highest viral titres in the affected animals (4).

Pulmonary intravascular macrophages (PIMs) are elements of the mononuclear phagocytic system (MPS) reported to occur in the lumina of pulmonary capillaries and arterioles in pigs, ruminants and felines (4–6, 8, 9).

The presence of PIMs endow the animals concerned with special features, both at the pulmonary and at the general level, which have been investigated by several authors; their occurrence has been related to the most common hydrodynamic pulmonary changes found in the species possessing them (2, 8, 9).

Six rabbits free from infectious and parasitic diseases were orally and parenterally inoculated with liver tissue extract from animals suffering from natural HVD and diagnosed by haemagglutination and electron microscopy.

Two days after inoculation, the animals were sacrificed after anaesthetization with ehter by vascular perfusion with 2% glutaraldehyde in phosphate buffer; once perfused, 1-mm^3 samples from the cranial, medial and caudal lobes were collected and fixed in the same medium, after which they were refixed in 2% osmium tetroxide and embedded in Durcupam ACM. 50-nm sections were stained with uranyl acetate and lead citrate, and then studied under a Philips CM-10 microscope at the Electron Microscopy Service of the University of Córdoba.

Bacterial clearance in rabbits reportedly occurs chiefly in the liver, spleen and marrow. However, some rabbits have been reported to undergo migration of Kupffer cells to the lungs on injection of colloid substances; this has also been reported to occur in cats on thorax ventilation, cells being later identified as PIMs (6).

The macrophages occurring in the alveolar capillaries of the inoculated rabbits showed the morphological features of PIMs reported by many authors (2, 7–9), namely uneven morphology, occurrence of pseudopodes and phagosomes, closeness to the vascular endothelium and, occasionally, linking modes to these cells.

Pulmonary intravascular erythrophagocytosis has been reported to occur in species with PIMs (1, 5, 7, 9), as has granulocyte phagocytosis on inoculation of bacteria (2), endotoxins (8) and viruses (7); according to some authors (2, 7–9), these cells play a major role in lung clearance. According to our own experience, most PIMs show

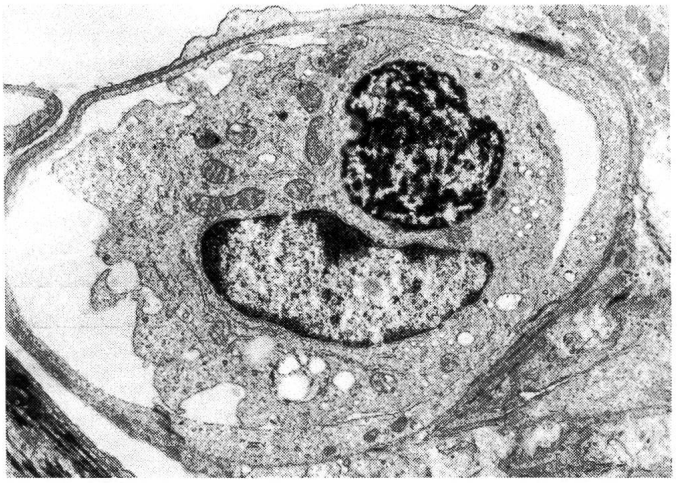

Fig. 1: Pulmonary intravascular macrophage with secondary lysosomes. X 15 000.

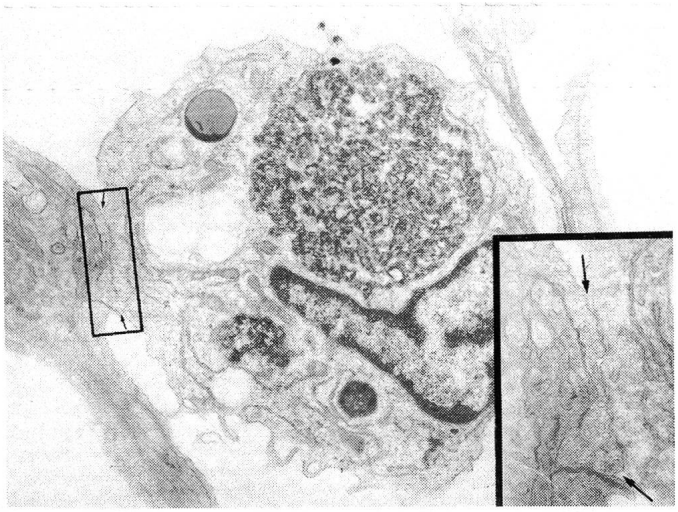

Fig. 2: Pulmonary intravascular macrophage. X15000. Insert: Intercellular junction of a pulmonary intravascular macrophage.